

Temperature dependence of the energy bandgap of multi-layer hexagonal boron nitride

X. Z. Du, J. Li, J. Y. Lin, and H. X. Jiang

Citation: *Appl. Phys. Lett.* **111**, 132106 (2017); doi: 10.1063/1.4994070

View online: <http://dx.doi.org/10.1063/1.4994070>

View Table of Contents: <http://aip.scitation.org/toc/apl/111/13>

Published by the [American Institute of Physics](#)

A dark blue banner with a network of glowing yellow and blue nodes and lines. The text 'Scilight' is in white and yellow. Below it, 'Sharp, quick summaries illuminating the latest physics research' is in white. A yellow button says 'Sign up for FREE!'. The AIP Publishing logo is in the bottom right.

Scilight

Sharp, quick summaries **illuminating**
the latest physics research

Sign up for **FREE!**

AIP
Publishing

Temperature dependence of the energy bandgap of multi-layer hexagonal boron nitride

X. Z. Du, J. Li, J. Y. Lin, and H. X. Jiang^{a)}

Department of Electrical and Computer Engineering, Texas Tech University, Lubbock, Texas 79409, USA

(Received 3 July 2017; accepted 14 September 2017; published online 28 September 2017)

The temperature dependence of the energy bandgap of hexagonal boron nitride (*h*-BN) has been probed via photoluminescence emission characteristics of a donor-to-acceptor pair transition in a 20-layer *h*-BN epilayer. The results indicate that the universal behavior of bandgap decreasing with temperature is absent in multi-layer *h*-BN. Below 100 K, the bandgap energy variation with temperature, E_g vs. T , is dominated by the electron-phonon coupling and conforms to the common behavior of redshift with an increase in temperature. At $T > 100$ K, the bandgap shows an unusual blueshift with temperature, which can be attributed to the unique behavior of the in-plane thermal expansion coefficient of *h*-BN that becomes negative above around 60 K. Although both graphite and *h*-BN have negative thermal expansion coefficients in a broad temperature range, graphite has a zero energy bandgap, which makes *h*-BN a unique semiconductor to exhibit this unusual temperature dependence of the energy bandgap. *Published by AIP Publishing.* <https://doi.org/10.1063/1.4994070>

Hexagonal boron nitride (*h*-BN), the only III-nitride wide bandgap semiconductor family member with a layered lattice structure, has been under intensive investigation in recent years. It is a promising material for deep ultraviolet optoelectronic devices^{1–13} due to its wide energy bandgap (~ 6.5 eV), high optical emission efficiency, high chemical and temperature stability, and large in-plane thermal conductivity. Another startling recent development is the neutron detectors with high efficiency based on B-10 enriched *h*-BN epilayers,^{14–16} which have demonstrated the highest thermal neutron detection efficiency to date among solid-state detectors at about 53%.^{15,16} However, a number of basic properties of *h*-BN are still unknown. For instance, the temperature variation of the energy bandgap, E_g vs. T , in *h*-BN has not been well studied, despite the fact that this relation is fundamentally important in terms of both fundamental understanding as well as practical applications of *h*-BN. A previous theoretical work has indicated that the variation of E_g with temperature in *h*-BN is weak attributing to the small indirect contribution of the lattice constant to the ionicity through crystal-field screening effects,¹⁷ inferring that it is challenging to measure such a dependence in *h*-BN. In the case of *h*-BN nanotubes, the temperature dependence of the excitonic emission peak exhibits a usual downshift in energy with temperature in the entire temperature range of 10–800 K.¹⁸ Nevertheless, it has not been possible to probe the general behavior of E_g vs. T in *h*-BN bulk crystals or epilayers. This is primarily due to the fact that the excitonic emission lines in *h*-BN bulk crystals generally exhibit complex features, whose linewidths are broadened and emission intensities drop rapidly at higher temperatures.^{6–8} On the other hand, *h*-BN epilayers with best optical qualities produced to date exhibit pure free exciton emission only at low temperatures.⁹

A set of *h*-BN epilayers with varying layer numbers has been synthesized by metal-organic chemical vapor deposition (MOCVD) on sapphire substrates.¹⁹ As shown in Fig. 1(a), these samples exhibit predominantly two near

band-edge emission lines (e.g., near 5.420 eV and 5.587 eV at 10 K for the 20-layer sample) at 10 K. Due to the fact that these two emission lines share similar spectroscopic features and that the observed energy separation is independent of the number of layers as well as coincides with the in-plane phonon vibration mode, E_{2g} , having an energy of 1370 cm^{-1} (~ 171 meV), we attributed these emission lines to a donor-acceptor-pair (DAP) transition and its one E_{2g} phonon replica, respectively.¹⁹ In this work, we have shown that the energy positions of these two near band-edge emission lines in multi-layer *h*-BN exhibit a systematic dependence on temperature, which enabled us with an unprecedented opportunity to study the E_g vs T relation in *h*-BN. A frequency quadrupled Ti:sapphire laser with wavelength of 195 nm and optical power of ~ 1 mW was used as the excitation source.¹¹ The PL signal was dispersed by a 1.3 m monochromator and then collected by a microchannel plate photo-multiplier tube.

A detailed study was carried out for the 20-layer *h*-BN. The near band-edge PL spectra of this sample were measured at a temperature range from 10 to 350 K, as shown in Fig. 1(b). The emission peaks (E_p) of the DAP transition and its one E_{2g} phonon replica (at 5.420 eV and 5.587 eV at 10 K, respectively) are clearly resolved. However, both emission peaks exhibit a similar but very unusual temperature dependence, i.e., E_p exhibits a downshift with increasing temperature up to 100 K and then upshift with increasing temperature above 100 K. This temperature dependence is distinctively different from the universal behavior of most other semiconductors including GaN and AlN²⁰ as well as from *h*-BN nanotubes.¹⁸ The spectral peak positions (E_p) of the near band-edge transitions in most semiconductors generally exhibit redshifts with increasing temperature, and the temperature variation of E_p follows approximately the Varshni empirical equation describing the temperature dependent bandgap in semiconductors

$$E_g(T) = E_g(0) - \alpha T^2 / (\beta + T), \quad (1)$$

^{a)}hx.jiang@ttu.edu

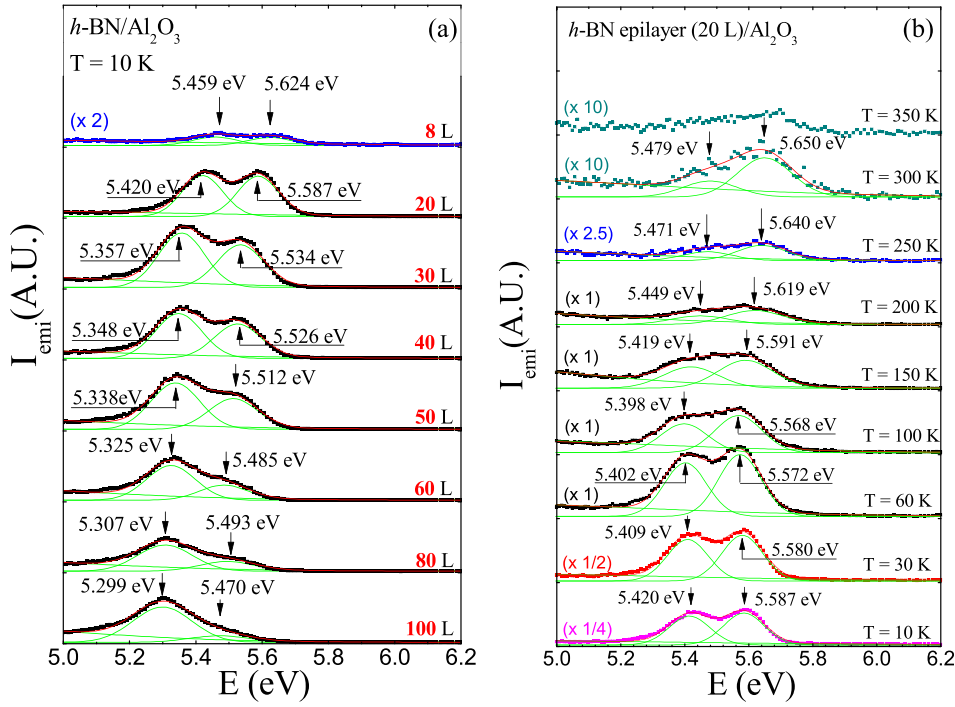


FIG. 1. (a) 10 K near band-edge PL spectra of *h*-BN epilayers with varying number of layers. The energy peak positions of the dominant emission lines are near 5.420 eV and 5.587 eV at 10 K for a 20-layer sample. (b) Near band-edge PL spectra of a 20-layer *h*-BN measured at different temperatures from 10 to 350 K.

where $E_g(0)$ is the energy bandgap at 0 K, and α and β are the Varshni coefficients.²¹

Figure 2(a) plots the temperature dependence of the two dominant emission line peak positions in the 20-layer *h*-BN sample. The linewidth broadening with increasing temperature along with reduced PL emission intensity prevented data collection at temperatures above 350 K. The energy difference between these two emission peaks (ΔE_p) as a function of temperature is plotted in Fig. 2(b), which clearly reveals that ΔE_p is independent of temperature and has an average value of 170.4 ± 0.3 meV, despite the fact that both emission peaks exhibit an unusual temperature dependence. This value of ΔE_p energy is very close to the in-plane phonon of E_{2g}

vibration mode (1370 cm^{-1}).^{22,23} The results further support our previous identification that these two emission lines have the same physical origin and one is a phonon replica of the other. In the case here, it is obvious that the 5.420 eV (@ 10 K) line is the zero phonon line (ZPL or $n=0$ line), whereas the 5.587 eV (@ 10 K) line is its one phonon replica ($n=1$ line). Another interesting feature shown in Fig. 1(b) is that the ratio of the emission intensity of the $n=1$ line to that of the ZPL increases with increasing temperature. The relative emission intensity of the $n=1$ line ($E_p \sim 5.587 \text{ eV}$ @ 10 K) to $n=0$ line ($E_p \sim 5.420 \text{ eV}$ @ 10 K) depends on the carrier-phonon coupling strength or the Huang–Rhys factor S .^{24,25} The relationship between the emission intensities of the n th phonon replica line (I_n) and $n=0$ line (I_0) follows, $I_n = I_0 \times \frac{S^n}{n!}$.^{24,25} For $n=1$ phonon replica line

$$S = I_1/I_0. \quad (2)$$

As clearly seen from Fig. 2(c) that the carrier-phonon coupling strength or the Huang–Rhys factor S is enhanced at higher temperatures. Such a behavior has been observed in nanofiber films.²⁶ It should be noted that the S factor is enhanced in thin *h*-BN epilayers and decreases almost linearly with an increase of the layer number,¹⁹ making the one-phonon replica line ($E_p \sim 5.587 \text{ eV}$ @ 10 K) undetectable in bulk *h*-BN as S approaches to zero.

For a clear presentation, Fig. 3 replots the evolution of E_p with temperature for the ZPL (the emission line with a peak position at 5.420 eV at 10 K). Two distinctive temperature regions are more clearly revealed; i.e., E_p shows a typical red-shift with increasing temperature at $T < 100$ K and an unusual blue-shift with temperature at $T > 100$ K. As a DAP transition, neglecting the Coulomb's interaction between donors and acceptors, its emission energy peak position can be described as $E_p = h\nu = E_g - E_D - E_A$, where E_D and E_A are the energy levels of the involved donor and acceptor, respectively. Using the Varshni's equation of Eq. (1) for E_g

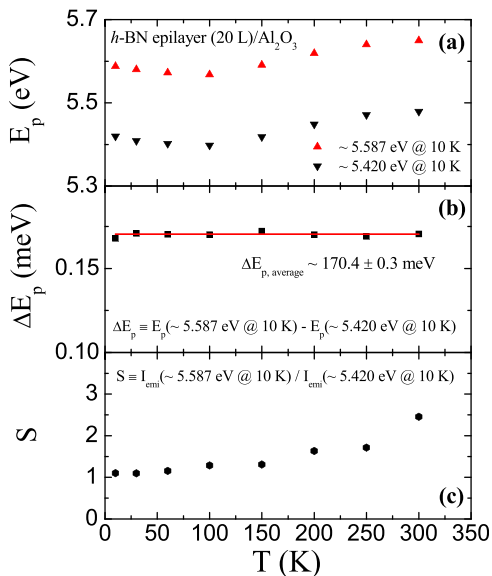


FIG. 2. Variations with temperature observed in a 20-layer *h*-BN for (a) the energy peak positions of the one-phonon replica emission line ($\sim 5.587 \text{ eV}$ @ 10 K) and zero phonon emission line ($\sim 5.420 \text{ eV}$ @ 10 K), (b) the energy difference between these two emission lines, and (c) Huang-Rhys factor S .

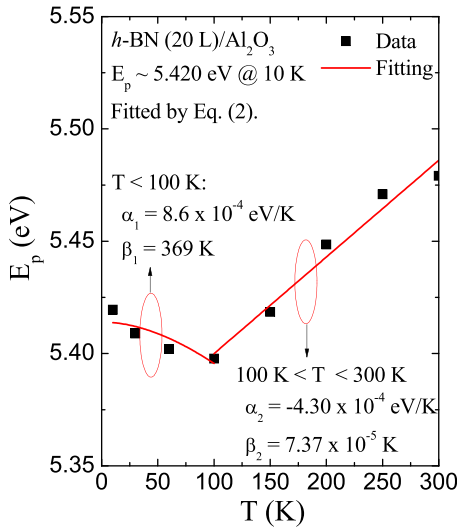


FIG. 3. Temperature dependence of the energy peak position of the zero phonon emission line (~ 5.420 eV @ 10 K) observed in a 20-layer *h*-BN fitted with Varshni's formula.

and neglecting the temperature dependence of E_A and E_D , the peak position E_p of the ZPL can be written as

$$E_p(T) = E_g(0) - E_D - E_A - \alpha T^2 / (\beta + T). \quad (3)$$

Therefore, the temperature evolution of E_p is expected to mimic that of E_g . In general, two dominant mechanisms are responsible for the energy bandgap variation (typically bandgap shrinkage) of semiconductors: (1) lattice constant dilation and (2) electron-phonon interaction. In Fig. 3, the solid curves are the least squares fitting of data with Eq. (3), however, in two different temperature regions. In the region of $T < 100$ K, E_g vs T (or E_p vs T) follows the anticipated trend, i.e., the bandgap decreases with increasing temperature and the temperature coefficient α is positive. As indicated in Fig. 2(c), the electron-phonon coupling strength S increases continuously with increasing temperature. Therefore, the temperature dependent electron-phonon interaction explains satisfactorily the variation of E_g with temperature at $T < 100$ K. The fitted value of α is 7.0×10^{-4} eV/K. The fitted value of α/β is $1.97 \mu\text{eV}/\text{K}^2$, which is larger compared with 1.28,²⁰ 1.06,²⁰ and $0.912 \mu\text{eV}/\text{K}^2$ (Ref. 27) for AlN, GaN, and InN, respectively. The comparison results are summarized in Table I. The value of β is associated with the Debye temperature of the crystal. Its fitted value is ~ 356 K, agrees reasonably well with a literature value of 400 K.²⁸ The results are an indication of a stronger electron-phonon interaction in *h*-BN in comparison with other III-nitride semiconductors. This is expected since one of the well-known effects of reduced

TABLE I. Comparison of bandgap parameters of α/β of *h*-BN epilayers of this work with other wurtzite III-nitride semiconductors.

	α/β ($\mu\text{eV}/\text{K}^2$)	References
<i>h</i> -BN(0–100 K)	1.97	This work
w-AlN	1.28	20
w-GaN	1.06	20
w-InN	0.912	27

dimensionality is the enhanced carrier-phonon interaction in 2D over that in 3D semiconductors, given the fact that *h*-BN used in this study only has 20 layers and that *h*-BN is a layered material naturally possessing 2D nature.

However, as shown in Fig. 3, E_p surprisingly increases with increasing temperature at $T > 100$ K, a behavior which is distinctively different from most semiconductors. Apparently this unique feature does not arise from the enhanced electron-phonon interaction at higher temperature, which tends to reduce E_g . Thus, it is most likely the lattice constant change with temperature that accounts for this distinctive behavior. As a semiconductor with layered structure, the interaction between layers of *h*-BN is through van der Waals force, which is very weak in comparison with in-plane interaction. As such, E_g of *h*-BN is predominantly determined by the energy difference between electrons localized on B and N atoms.²⁹ Therefore, the temperature dependent E_g of *h*-BN at $T > 100$ K can be attributed primarily to the in-plane lattice constant change with temperature. The in-plane lattice constants (a) of *h*-BN at different temperatures have been previously measured by Paszkowicz *et al.*,³⁰ and the results are reproduced in Fig. 4(b). The results shown in Fig. 4(b) reveal that the in-plane lattice constant expands slightly at low temperatures and then shrinks continuously with increasing temperature at $T \geq 70$ K.³⁰ The calculated values of the in-plane thermal expansion coefficients of *h*-BN, α_a , are also re-plotted in Fig. 4(c),³⁰ which show that they are positive at low temperatures and become negative at temperatures above ~ 60 K. The results presented in Figs. 4(b) and 4(c) indicate that the in-plane lattice constant of *h*-BN decreases with increasing temperature from ~ 70 to 300 K. In this temperature region, E_g of *h*-BN epilayers

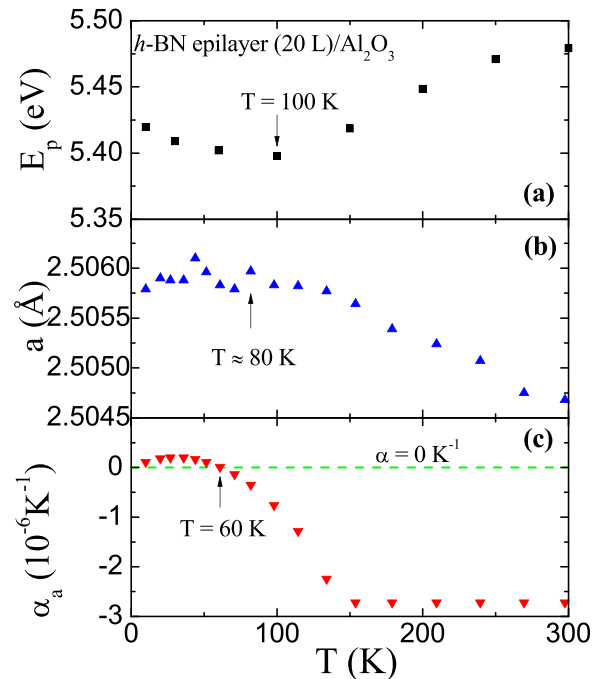


FIG. 4. Variations with temperature of (a) the energy peak position of the zero phonon emission line (~ 5.420 eV @ 10 K) observed in a 20-layer *h*-BN, (b) in-plane lattice constant obtained experimentally [data reproduced with permission from Paszkowicz *et al.*, Appl. Phys. A **75**, 431 (2002). Copyright 2001 Springer-Verlag³⁰], and (c) calculated thermal expansion coefficient of *h*-BN [data reproduced with permission from Paszkowicz *et al.*, Appl. Phys. A **75**, 431 (2002). Copyright 2001 Springer-Verlag³⁰].

is determined by two competing mechanisms: (1) reduced in-plane lattice constant which tends to increase E_g , and (2) enhanced electron-phonon interaction which is inclined to decrease E_g . From ~ 70 to ~ 100 K, E_g still exhibits a redshift with increasing temperature, indicating that the latter mechanism is still prevailing. However, E_g shows a blueshift with increasing temperature above 100 K, revealing that the temperature dependence of E_g above 100 K is dominated by the effect of reduction in the in-plane lattice constant at higher temperatures. The slope of E_p versus T is about 0.43 meV/K from 100 to 300 K as fitted in Fig. 3, which means that the temperature coefficient of E_g , or the Varshni coefficient $\alpha = -0.43$ meV/K.

It is interesting to note that in the case of *h*-BN nanotubes, the excitonic emission peak exhibits a universal downshift in energy with increasing temperature in the entire temperature range of 10–800 K, in contrast with the results obtained for thin *h*-BN epilayers here. This situation seems analogous to the temperature dependence of the effective energy bandgap of suspended carbon nanotubes,^{31,32} which shifts down in energy with increasing temperature despite the fact that the thermal expansion of graphite has a negative coefficient in the same temperature range. It was shown that the temperature dependence of the optical transition energies of carbon nanotubes is dominated by the effect of electron-phonon coupling.^{31,32} Based on these observations, we speculate that the temperature dependence of the bandgap of *h*-BN nanotube follows a similar trend as that of carbon nanotubes and is dominated by the electron-phonon coupling in the entire temperature range. It is tantalizing to say that the temperature dependence of the bandgap of multi-layer *h*-BN should be similar to that of graphite since both materials have negative thermal expansion coefficients in a broad temperature range, except that graphite has a zero energy bandgap. In this sense, multi-layer *h*-BN represents a unique semiconductor to exhibit this unusual temperature dependence of the energy bandgap.

In summary, we report on the studies of the bandgap variation with temperature in multi-layer *h*-BN by following the temperature dependence of the energy peak position of a donor-acceptor pair emission line. At temperatures below 100 K, the bandgap energy exhibits a usual downshift with increasing temperature and the temperature dependence is dominated by electron-phonon coupling. At temperatures above 100 K, the bandgap energy exhibits an unusual upshift with increasing temperature. This unique feature can be accounted for by the unusual in-plane thermal expansion coefficient of *h*-BN, which is negative above ~ 70 K.

The effort on the fundamental optical studies of *h*-BN was supported by ARO and monitored by Dr. Michael Gerhold (W911NF-16-1-0268) and *h*-BN growth was partially supported

by the DOE NNSA SSAA program (DE-NA0002927). Jiang and Lin are grateful to the AT&T Foundation for the support of Ed Whitacre and Linda Whitacre endowed chairs.

- ¹B. Arnaud, S. Lebègue, P. Rabiller, and M. Alouani, *Phys. Rev. Lett.* **100**, 189702 (2008).
- ²L. Wirtz, A. Marini, and A. Rubio, *Phys. Rev. Lett.* **96**, 126104 (2006).
- ³L. Museur and A. Kanaev, *J. Appl. Phys.* **103**, 103520 (2008).
- ⁴Y. Kubota, K. Watanabe, O. Tsuda, and T. Taniguchi, *Science* **317**, 932 (2007).
- ⁵K. Watanabe, T. Taniguchi, and H. Kanda, *Nat. Photonics* **3**, 591 (2009).
- ⁶K. Watanabe and T. Taniguchi, *Phys. Rev. B* **79**, 193104 (2009).
- ⁷K. Watanabe and T. Taniguchi, *Int. J. Appl. Ceram. Technol.* **8**, 977 (2011).
- ⁸X. K. Cao, B. Clubine, J. H. Edgar, J. Y. Lin, and H. X. Jiang, *Appl. Phys. Lett.* **103**, 191106 (2013).
- ⁹X. Z. Du, J. Li, J. Y. Lin, and H. X. Jiang, *Appl. Phys. Lett.* **108**, 052106 (2016).
- ¹⁰R. Dahal, J. Li, S. Majety, B. N. Pantha, X. K. Cao, J. Y. Lin, and H. X. Jiang, *Appl. Phys. Lett.* **98**, 211110 (2011).
- ¹¹S. Majety, X. K. Cao, J. Li, R. Dahal, J. Y. Lin, and H. X. Jiang, *Appl. Phys. Lett.* **101**, 051110 (2012).
- ¹²S. Majety, J. Li, X. K. Cao, R. Dahal, B. N. Pantha, J. Y. Lin, and H. X. Jiang, *Appl. Phys. Lett.* **100**, 061121 (2012).
- ¹³J. Li, S. Majety, R. Dahal, W. P. Zhao, J. Y. Lin, and H. X. Jiang, *Appl. Phys. Lett.* **101**, 171112 (2012).
- ¹⁴J. Li, R. Dahal, S. Majety, J. Y. Lin, and H. X. Jiang, *Nucl. Instrum. Methods A* **654**, 417 (2011).
- ¹⁵A. Maity, T. C. Doan, J. Li, J. Y. Lin, and H. X. Jiang, *Appl. Phys. Lett.* **109**, 072101 (2016).
- ¹⁶A. Maity, S. J. Grenadier, J. Li, J. Y. Lin, and H. X. Jiang, *Appl. Phys. Lett.* **111**, 033507 (2017).
- ¹⁷A. Zunger, A. Katzir, and A. Halprin, *Phys. Rev. B* **13**, 5560 (1976).
- ¹⁸X. Z. Du, C. D. Frye, J. H. Edgar, J. Y. Lin, and H. X. Jiang, *J. Appl. Phys.* **115**, 053503 (2014).
- ¹⁹X. Z. Du, M. R. Uddin, J. Li, J. Y. Lin, and H. X. Jiang, *Appl. Phys. Lett.* **110**, 092102 (2017).
- ²⁰K. B. Nam, J. Li, J. Y. Lin, and H. X. Jiang, *Appl. Phys. Lett.* **85**, 3489 (2004).
- ²¹Y. P. Varshni, *Physica* **34**, 149 (1967).
- ²²R. J. Nemanich, S. A. Solin, and R. M. Martin, *Phys. Rev. B* **23**, 6348 (1981).
- ²³R. V. Gorbachev, I. Riaz, R. R. Nair, R. Jalil, L. Britnell, B. D. Belle, E. W. Hill, K. S. Novoselov, K. Watanabe, T. Taniguchi, A. K. Geim, and P. Blake, *Small* **7**, 465 (2011).
- ²⁴B. Di Bartolo and R. Powell, *Phonons and Resonances in Solids* (Wiley, New York, 1976), Chap. 10.
- ²⁵K. W. Böer, *Survey of Semiconductor Physics* (Van Nostrand Reinhold, New York, 1990), Chap. 20.
- ²⁶F. Balzer, A. Pogantsch, and H.-G. Rubahn, *J. Lumin.* **129**, 784 (2009).
- ²⁷T. D. Veal, C. F. McConville, and W. J. Schaff, *Indium Nitride and Related Alloys* (CRC Press, Boca Raton, 2009), p. 247.
- ²⁸See <http://www.ioffe.ru/SVA/NSM/Semicond/BN/basic.html> for Debye temperature of *h*-BN.
- ²⁹G. W. Semenoﬀ, *Phys. Rev. Lett.* **53**, 2449 (1984).
- ³⁰W. Paszkowicz, J. B. Pelka, M. Knapp, T. Szyszko, and S. Podsiadlo, *Appl. Phys. A* **75**, 431 (2002).
- ³¹R. B. Capaz, C. D. Spataru, P. Tangney, M. L. Cohen, and S. G. Louie, *Phys. Rev. Lett.* **94**, 036801 (2005).
- ³²S. B. Cronin, Y. Yin, A. Walsh, R. B. Capaz, A. Stolyarov, P. Tangney, M. L. Cohen, S. G. Louie, A. K. Swan, M. S. Ünlü, B. B. Goldberg, and M. Tinkham, *Phys. Rev. Lett.* **96**, 127403 (2006).